ADVANCED MATERIALS

Supporting Information

for *Adv. Mater.*, DOI: 10.1002/adma.201802061

Two-Dimensional Antimonene-Based Photonic Nanomedicine for Cancer Theranostics

*Wei Tao, Xiaoyuan Ji, Xianbing Zhu, Li Li, Junqing Wang, Ye Zhang, Phei Er Saw, Wenliang Li, Na Kong, Mohammad Ariful Islam, Tian Gan, Xiaowei Zeng, Han Zhang, Morteza Mahmoudi, Guillermo J. Tearney, and Omid C. Farokhzad**

Supporting Information

Two-Dimensional Antimonene-based Photonic Nanomedicine for Cancer Theranostics

*Wei Tao, Xiaoyuan Ji, Xianbing Zhu, Li Li, Junqing Wang, Ye Zhang, Phei Er Saw, Wenliang Li, Na Kong, Mohammad Ariful Islam, Tian Gan, Xiaowei Zeng, Han Zhang, Morteza Mahmoudi, Guillermo J. Tearney, Omid C. Farokhzad**

Experimental Section

Materials. Doxorubicin (DOX), chloroform, dimethyl sulphoxide (DMSO), Cy 5.5-NHS, and ethanol were purchased from Sigma-Aldrich (St. Louis, MO. USA). 1,2-Distearoyl-sn-glycero-3-phosphoethanolamine-N-[methoxy(poly ethylene glycol)-3000] (DSPE-PEG_{3k}) was obtained from Avanti Polar Lipids, Inc. DSPE-PEG_{3k}-NH_2 were purchased from Nanocs Inc. (New York, USA). Calcein-AM and PI were bought from Invitrogen (USA). PBS (pH 7.4), fetal bovine serum (FBS), DMEM, RPMI, trypsin-EDTA and penicillin-streptomycin were purchased from Gibco Life Technologies (AG, Switzerland). Antibodies against Arf-6, Flotillin, RhoA, Cdc42, caveolin, EEA1 and clathrin were from Cell Signaling Technology, Inc. (Beverly, MA, USA). Antibody against LAMP1 was from Santa Cruz Biotechnologies (CA, USA), and DAPI was from Sangon Biotech (Shanghai, China).

Synthesis of AM NSs and surface coating of DSPE-PEG. AM NSs were prepared by a modified liquid-phase exfoliation method with probe sonication in ethanol, based on a reported method[1]. First, commercial antimony powder with initial concentration of 20 mg/mL was dispersed in ethanol. The solution was then sonicated for 8 h in an ice bath at 500 W and centrifuged at 3,000 rpm for 10 min to discard the un-exfoliated bulk antimony. Finally, the suspensions were then centrifuged at 10,000 rpm for 30 min and the precipitates collected for future use. For PEG functionalization, 10 mg of AM NSs was dispersed in 100 mL chloroform with pre-dissolved 50 mg DSPE-PEG. After ultra-sonication for 10 min in an ice bath,

chloroform was removed by vacuum rotary evaporation. The AM-PEG NSs samples were dissolved in water, centrifuged at 14,000 rpm, and washed with DI water three times to remove the unbound DSPE-PEG. The final AM-PEG NSs samples were re-suspended in water and stored at 4 ^{o}C for future use.

Preparation of AM-PEG/DOX NSs. For DOX loading, the prepared AM-PEG NSs were dispersed into phosphate-buffered saline (PBS) and then mixed with different concentrations of free DOX solution to final concentrations of 0.2, 0.4, 0.6, 0.8, and 1 mg/mL. The mixtures were stirred for 24 h at room temperature and centrifuged at 10,000 rpm for 10 min and washed with DI water three times to remove the unbound excess DOX. The resulting AM-PEG/DOX NSs were re-dispersed in water and stored at 4 ^{o}C. The amount of loaded DOX was determined according to the absorbance peak of AM-PEG/DOX NSs at 490 nm. Cy5.5-loaded AM-PEG NSs were prepared using a similar method.

Characterization of AM-based NSs. Transmission electron microscopy (TEM, JEM-2100UHR, JEOL, Japan) and atomic-force microscopy (AFM, FASTSCANBIO, Germany) were applied to characterize the morphology, size, and thickness of the AM NSs and AM-PEG NSs. The chemical compositions of the AM NSs or AM-PEG NSs were analyzed by X-ray photoelectron spectroscopy (XPS, ESCALAB 250Xi, Japan) and Fourier transform infrared spectrophotometry (FTIR, Nexus 470, Nicolet, Madison, WI, USA) Elemental mapping was carried out using an energy-dispersive X-ray spectroscope (EDS) (Inca X-MAX, Oxford, UK), which was directly connected to a scanning electron microscope (JSM-7001F). The distribution of elements on the AM NSs, AM-PEG NSs, and AM-PEG/DOX NSs was mapped. UV-Vis-NIR spectra were obtained on an Infinite M200 PRO spectrophotometer. The chemical structures of the AM NSs and AM-PEG NSs were analyzed by X-ray diffraction (XRD) patterns recorded on a Bruker D8

multipurpose XRD system and Raman spectrum obtained by Aramis made by HORIBA JOBIN YVON.

Photothermal performance of AM-PEG NSs. To measure the light-to-heat conversion performance of the AM-PEG NSs, 1 mL AM-PEG NSs aqueous dispersions with different concentrations (0-200 μg/mL) were introduced into a quartz cuvette and exposed to an 808-nm NIR laser at a power density of 1, 1.5, or 2 W/cm^2 for 5 min. The temperature change of the AM-PEG NSs aqueous solution was recorded using an IR thermal camera (TI100 Infrared Camera FLK-TI100 9HZ, FLUKE).

pH-/NIR-responsive release of DOX from AM-PEG/DOX NSs. To assess DOX release kinetics, 1 mL of AM-PEG/DOX NSs solution was put into a dialysis bag (MWCO = 14 kDa) and incubated in 9 mL PBS at one of two different pHs (pH = 7.4 or 5.0). 0.1 mL of the solution outside the dialysis bag was collected to detect absorbance at 490 nm to determine the concentrations of released drug. To study NIR-triggered release of DOX, the processes were carried out under the same conditions at pH =7.4 and 5.0, and exposed to an 808 nm NIR laser at a power density of 0.8 W/cm^2 over a period of 10 min with 0, 2, 4, 6, 8, and 12 h incubation.

***In vitro* biocompatibility assay of AM-PEG NSs.** The cytotoxicity of AM-PEG NSs was assessed through testing the viability of normal cells and cancer cells treated with AM-PEG NSs by Alamar Blue assay. Briefly, five different cell lines (HEK293, HeLa, PC3, A549, and MCF-7) were incubated in the culture medium at 37 ^{o}C in an atmosphere of 5% CO_2 for 24 h. Subsequently, fresh culture medium pre-dissolving AM-PEG NSs with different concentrations (0-200 μg/mL) was used to replace the old culture medium, and incubation was continued for another 24 h. Finally, cell viabilities were determined by Alamar Blue assay after washing with

PBS relative to the control cells incubated with the same volume of culture medium without AM-PEG NSs.

Immunofluorescence assay for intracellular fate of AM-based NSs. MCF-7 cells treated with 40 μg/mL Cy5.5-labeled AM-PEG (AM-PEG-Cy5.5) NSs for 4 h and fixed in 4% paraformaldehyde. Then the cells were blocked using 3% BSA and incubated with the following primary antibodies: EEA1, Clathrin, Arf-6, flotillin, Cdc42, RhoA, EEA1, Caveolin, Rab34, and LAMP-1 as indicated. TRITC and FITC-labeled secondary antibodies were used to detect the primary antibody.

Pearson's Correlation Coefficient analysis. The software ImageJ was applied to analyze the pixel intensity of each image, and then Pearson's correlation coefficient was further analyzed.

***In vitro* tumor-penetration assays.** MCF-7 three-dimensional (3D) multicellular tumor spheroids were established based on a previously reported method[2]. MCF-7 cells (2×10^3) were seeded in a 96-well plate pre-coated with 50 μL low-melting-point agarose (1.5%). The 3D MCF-7 tumor spheroids were treated with AM-PEG/DOX NSs ([AM] = 50 μg/mL, [DOX] = 50 μg/mL) for 1 h after 7 days' growth. One group of the treated MCF-7 tumor spheroids was irradiated under an 808-nm laser (0.8 W/cm^2) for 5 min and incubated for another 3 h (with-laser group). The other group was simply incubated for another 3 h (without-laser group). After the different treatments, MCF-7 tumor spheroids were rinsed with PBS three times and fixed with paraformaldehyde (4%) for 30 min. CLSM images were taken to assess the fluorescence intensity of MCF-7 tumor spheroids at different depths.

Photo-induced cell uptake assay. To determine the photo-induced cell uptake of AM-PEG/DOX NSs, 2×10^4 MCF-7 cells were seeded on coverslips in 24-well plates for 24 h

incubation before the addition of AM-PEG/DOX NSs ([AM] = 50 μg/mL, [DOX] = 50 μg/mL). After 10 min incubation with/without NIR laser irradiation (0.5 W/cm^2), all cells were incubated in fresh media for another 4 h, then fixed and stained with DAPI for nuclei staining according to the standard protocol. CLSM images were then taken.

***In vitro* combined therapy using AM-PEG/DOX NSs.** To test the *in vitro* anticancer effects of AM-PEG/DOX NSs, the viability of MCF-7 and PC3 cells was measured after treatment with AM-PEG NSs (50 μg/mL), DOX (50 μg/mL), or AM-PEG/DOX NSs ([AM]= 50 μg/mL, [DOX] = 50 μg/mL). After being cultured for 1 h, the NIR-alone group, the PTT group (AM-PEG NSs + NIR), and the chemo-PTT combined therapy group (AM-PEG/DOX NSs + NIR) continued to be irradiated with an 808-nm NIR laser (0.8 W/cm^2) for 5 min. After that, the culture medium in all groups (*i.e.*, control, NIR alone, AM-PEG alone, DOX alone, PTT, AM-PEG/DOX, and chemo-PTT combined therapy) was removed and cells were rinsed three times with PBS. Fresh complete medium was then added to the wells and all cells were incubated for another 24 h. Lastly, Alamar Blue assay was used to evaluate cell viability.

Xenograft Tumor model. Healthy athymic nude mice were purchased from Charles River Laboratories. All *in vivo* studies were performed in accordance with National Institutes of Health animal care guidelines and in strict pathogen-free conditions in the animal facilities of Brigham and Women's Hospital. The animal protocol was approved by the Institutional Animal Care and Use Committees at Harvard Medical School. To build the xenograft tumor models, 100 μL of MCF-7 cells (Density: 2×10^6) was suspended in serum-free cell medium and implanted subcutaneously in female nude Balb/c mice. Tumor volume was calculated by "$V = 4\pi/3 \times (\text{tumor length}/2) \times (\text{tumor width}/2)^2$" using a Vernier caliper. The mice were used for further experiments when the tumor had grown to ~100 mm^3 in diameter.

Pharmacokinetic studies. To study the pharmacokinetic profile *in vivo*, healthy Balb/c mice were divided in two groups with 5 mice in each group and intravenously (*i.v.*) injected with 200 μL of free DOX (6 mg/kg) or AM-PEG/DOX NSs ([AM]= 6 mg/kg, [DOX] = 6 mg/kg). At certain time intervals, 20 μL of blood was collected and dissolved in 300 μL of lysis buffer. The DOX was extracted by adding 300 μL of HCl/isopropanol to the mixture of lysis buffer and blood. After incubation in the dark for 12 h, the mixture was centrifuged to obtain the DOX in supernatant, and the amount of DOX remaining in blood was determined by absorbance at 490 nm.

Immunofluorescence staining for *in vivo* penetration studies

MCF-7 tumor-bearing male BALB/c nude mice were randomly divided into two groups (n = 3) and all animals were *i.v.*-injected with Cy5.5-loaded AM-PEG NSs at 1 mg Cy5.5 dose per kg mouse weight. After 4 h of injection, one group of mice was irradiated with an 808 nm NIR laser (0.8 W/cm^2) for 10 min, and no further treatment was performed for the other group of mice. The mice in both groups were sacrificed after another 30 min, and the tumors were harvested, fixed with 4% paraformaldehyde, embedded in paraffin, and cut into sections. In order to stain the tumor vasculature, the slices were heated at 60 ^{o}C for 1 h and washed with xylene, ethanol, and PBS thrice. Afterwards, the slices were blocked with 10% FBS for 1.5 h and incubated with rat anti-mouse CD31 antibody (Abcam) at 4 ^{o}C for 1 h. After washing with PBS/0.2% triton X-100 thrice, the slices were stained by Alexa Flour 488-conjugated secondary antibody (Goat anti-rat IgG, Abcam) for 1 h. Thereafter, the slices were washed with PBS thrice and then stained with Hoechst 33342. An FLV1000 CLSM was used to take the images of the tumor vasculature.

***In vivo* fluorescence imaging and biodistribution analysis.** For *in vivo* fluorescence imaging and biodistribution analysis of these NSs, MCF-7 tumor-bearing female mice were given an *i.v.* injection of AM-PEG-Cy5.5 NSs (1 mg/kg equivalent Cy5.5 for each mouse) via tail vein. The mice were imaged using the Maestro2 In-Vivo Imaging System (Cri Inc) at 1, 2, 4, 8, 12, and 24 h post-injection. Furthermore, major organs (*e.g.*, heart, liver, spleen, lung, and kidney) or tumors were collected and imaged without delay. The accumulation of NSs in major organs or tumors was quantified by detecting the fluorescence intensity (a.u.) of Cy5.5 via ImageJ and then dividing by the weight (g) of each organ.

***In vivo* ultrasound and photoacoustic imaging.** For *in vivo* ultrasound (US) and photoacoustic (PA) imaging of the developed AM-PEG NSs, MCF-7 tumor-bearing female mice were given an *i.v.* injection of the NSs (at the AM dose of 3 mg/kg) *via* tail vein. 12 h after injection, the mice were sacrificed, the tumors harvested, and PA/US coregistered images were recorded by a PA instrument (LeSonics, Wellman Center of Photomedicine). BP-PEG NSs (with similiar size, thinkness, and shape) were developed according to our previous report[3] and selected as control PA agents. The software ImageJ was applied to analyze the PA signals in each region of interest (ROI).

***In vivo* antitumor efficacy.** For *in vivo* combined therapy, MCF-7 tumor-bearing mice were randomly divided into five groups (n = 5 per group) until the tumor volume reached ~100 mm^3. Different treatments were performed as follows: **1)** Group 1: *i.v.* injected with 200 μL of Saline, **2)** Group 2: *i.v.* injected with 200 μL of free DOX at a dose of 6 mg/kg, **3)** Group 3: *i.v.* injected with 200 μL of AM-PEG/DOX NSs ([AM]= 6 mg/kg, [DOX] = 6 mg/kg), **4)** Group 4: *i.v.* injected with 200 μL of AM-PEG NSs at the AM dose of 6 mg/kg and treated with NIR irradiation for 10 min (0.8 W/cm^2, 808 nm) at 12 h post-injection, and **5)** Group 5: *i.v.* injected with 200 μL of AM-PEG/DOX NSs ([AM]= 6 mg/kg, [DOX] = 6 mg/kg) and treated with NIR

irradiation for 10 min (0.8 W/cm^2, 808 nm) at 12 h post-injection. The date first treatment was performed is designated Day 0. Three more treatments were performed on Days 4, 8, and 12 for Groups 1 and 2. Two more treatments were performed on Days 4 and 8 for Group 3. There were no more treatments for Groups 4 and 5. Tumor sizes were measured with a caliper every other day for 14 days and calculated as volume. Relative tumor volumes were calculated as V/V_0 (V_0 was the tumor volume when the treatment was initiated).

To further compare the therapeutic efficacy of NSs with that of AM-based quantum dots[4], we intratumorally (*i.t.*) injected the therapeutics in all groups as follows: **1)** Group 1: 40 μL of Saline, **2)** Group 2: 40 μL of free DOX at a dose of 1 mg/kg, **3)** Group 3: 40 μL of AM-PEG/DOX NSs ([AM]= 1 mg/kg, [DOX] = 1 mg/kg), **4)** Group 4: *i.t.* 40 μL of AM-PEG NSs at the AM dose of 1 mg/kg and treated with NIR irradiation for 10 min (0.8 W/cm^2, 808 nm), and **5)** Group 5: 40 μL of AM-PEG/DOX NSs ([AM]= 1 mg/kg, [DOX] = 1 mg/kg) and treated with NIR irradiation for 10 min (0.8 W/cm^2, 808 nm). The date first treatment performed is designated as Day 0. Tumor sizes were measured with a caliper every other day for 14 days and calculated as volume. Relative tumor volumes were calculated as V/V_0.

Oxidative degradability of AM-based NSs. Two groups of freshly created AM NSs were incubated in water for different numbers of days (0, 2, 4, 6, 8, and 10) in either an oxygen atmosphere or an oxygen-free environment at 37 °C. At the designed time points, the photothermal effects (TI100 Infrared Camera FLK-TI100 9HZ, FLUKE) and the UV/Vis-NIR absorbance spectra (Infinite M200 PRO spectrophotometer) of the suspensions were tested. The color changes during the process were imaged, and the variation of the absorption ratios at 808 nm (A/A_0%) of the prepared AM NSs in water after different periods of incubation were recorded.

Metabolism of AM-based NSs *in vivo*. To assess the metabolism of AM-based NSs *in vivo* (retention or cleared/degraded), we further performed a long-term biodistribution study using inductively coupled plasma mass spectrometric (ICP-MS) analysis of antimony in different organs (*i.e.*, liver, spleen, kidney, heart, lung, stomach, intestine, skin, muscle, and bone). These organs, which were collected from mice *i.v.*-injected with AM-PEG NSs ([AM]= 6 mg/kg), were weighed and afterwards dissolved in aqua fortis. After heating for 4 h at 150 °C and cooling down to room temperature, the prepared samples were diluted to 10 mL using deionized water. The ICP-MS (Iris Advantage 1000, Thermo Jarrell Ash) was used to analyze and determine the total amount of antimony.

Histology. Healthy Balb/c mice were randomly divided into 3 groups (n = 5 per group) and subjected to different treatments: (i) control group without any treatment, (ii) AM-PEG/DOX NSs directly *i.v.* injected into the mice, and (iii) AM-PEG/DOX NSs *i.v.* injected into the mice after 808-nm irradiation for 10 min ([AM]= 6 mg/kg, [DOX] = 6 mg/kg). Immunohistochemical analyses were performed on major organs (*i.e.*, heart, liver, spleen, liver, and kidney) 1, 7, and 14 days post-injection.

Biocompatibility assessment of AM-based NSs *in vivo*. Blood biocompatibility was preliminarily evaluated by a complete blood panel test (CBPT) and serum biochemistry (SB). In brief, AM-PEG NSs (6 mg/kg) were *i.v.* injected into three groups of healthy Balb/c mice. Another five healthy Balb/c mice treated with PBS were used as controls. All five mice in each treatment group were sacrificed to collect blood for CBPT and SB test 1, 7, or 14 days after injection, respectively.

Statistical analysis. All results are reported as the mean ± S.E.M. and comparisons were performed using a two-tailed Student's t test. All experiments, unless otherwise stated, were

performed in triplicate. Statistical values are indicated in figures according to the following scale: * P<0.05, ** P<0.01 and *** P<0.001.

Results and discussion

In vitro biocompatibility of AM-PEG NSs.

After confirming the high light-to-heat conversion efficiency and superior photothermal effects of AM-PEG NSs, their biocompatibility was tested. To analyze the biocompatibility of AM-PEG NSs, the viability of normal and tumor cells, *i.e.*, Hek293 (normal human embryonic kidney cells), Hela (human cervical cancer cells), PC3 (human prostate cancer cells), A549 (human alveolar basal epithelial cells), and MCF-7 (human breast cancer cells), was tested after incubation with the AM-PEG NSs with different concentrations ranging from 25 to 200 μg/mL. As displayed in Figure S5c, there was no significant cytotoxicity among the five types of cells at our tested dose, suggesting good biocompatibility and suitability for biomedical applications.

Synergistic effect of the chemo-photothermal therapy strategy using AM-PEG/DOX NSs.

To further check whether the antitumor effect in Group 5 (Figure 5c) is additive or synergistic effect of chemotherapy and PTT, we utilized well-demonstrated methods to calculate the combination index[5]. In brief, the expected value of combination effect between treatment of chemotherapy and PTT is calculated as follow.

$$V_{exp} = \left(\frac{V_{G3}}{V_{Ctrl}}\right) \times \left(\frac{V_{G4}}{V_{Ctrl}}\right) \times V_{Ctrl} \quad (1)$$

where V_{exp} is the expected value of combination effect between treatment of chemotherapy and PTT, V_{Ctrl} is the observed value of control group (Group 1), V_{G3} is the observed value of chemotherapy treatment in Group 3, and V_{G4} is the observed value of PTT treatment in Group 4. The combination index is calculated as follow.

$$CI = \frac{V_{exp}}{V_{obs}} \quad (2)$$

where *CI* is combination index, and V_{obs} is the observed value of combination effect between treatment of chemotherapy and PTT in Group 5. $CI > 1$ indicates a synergistic effect, $CI = 1$ indicates an additive effect, and $CI < 1$ indicates an antagonistic effect. Based on the above principles, the expected volume on Day 14 (V_{exp}) is ≈86.14 mm^3 (*i.e.*, theoretically predicted value under additive effect), while the observed volume on Day 14 (V_{obs}) is ≈17.24 mm^3. Therefore, the *CI* value on the last day of treatment is calculated to be ≈4.997, indicating an efficient synergistic effect.

Discussion of the clinical translation potential of AM-based nanomedicines.

As antimonial drugs have been utilized in medicine for several centuries[6], the toxicity of antimony-based materials has been widely studied, which could prove useful for our novel application of AM-based NSs. For example, there was no manifestation of toxicity in rats at a dose of 0.1 to 4.0 mg/kg antimony compounds taken orally over a period of 3.5 months[7]. Nor was any adverse effect observed in a 91-day study in which rats were orally administered two antimony-containing pigments at dosages of 36 and 22 mg/kg, respectively[8]. Even consumption of 100 mg/kg Sb^{3+} or Sb^{5+} oxides by cats and dogs for several months elicited no toxic effect, according to Elinder and Frieberg[9]. The lambs of ewes that were administered antimony compounds at 2.0 mg/kg for 45 days or throughout gestation showed no developmental effects[10]. No abnormalities in fetuses were found after five intramuscular injections of Sb^{5+} to Wistar rats during gestation[11] or of antimony trioxide to rats[11]. Given what we know about the history of antimonial drugs, we believe that these newly developed AM-PEG NSs might be easier or more likely to be clinically translatable as nanomedicines (*e.g.*, both drug delivery and photothermal agents) than other 2D nanomaterials. However, the premise of biocompatibility and safety is strictly connected to a certain dose: the median lethal dose (LD_{50}) for antimony trioxide (calculated as Sb^{3+}) has been reported to be 209 mg/kg and that of antimony oxide 978

mg/kg [12]. Therefore, many systemic dose-dependency studies still need to be carried out before clinical experiments using these AM-PEG NSs.

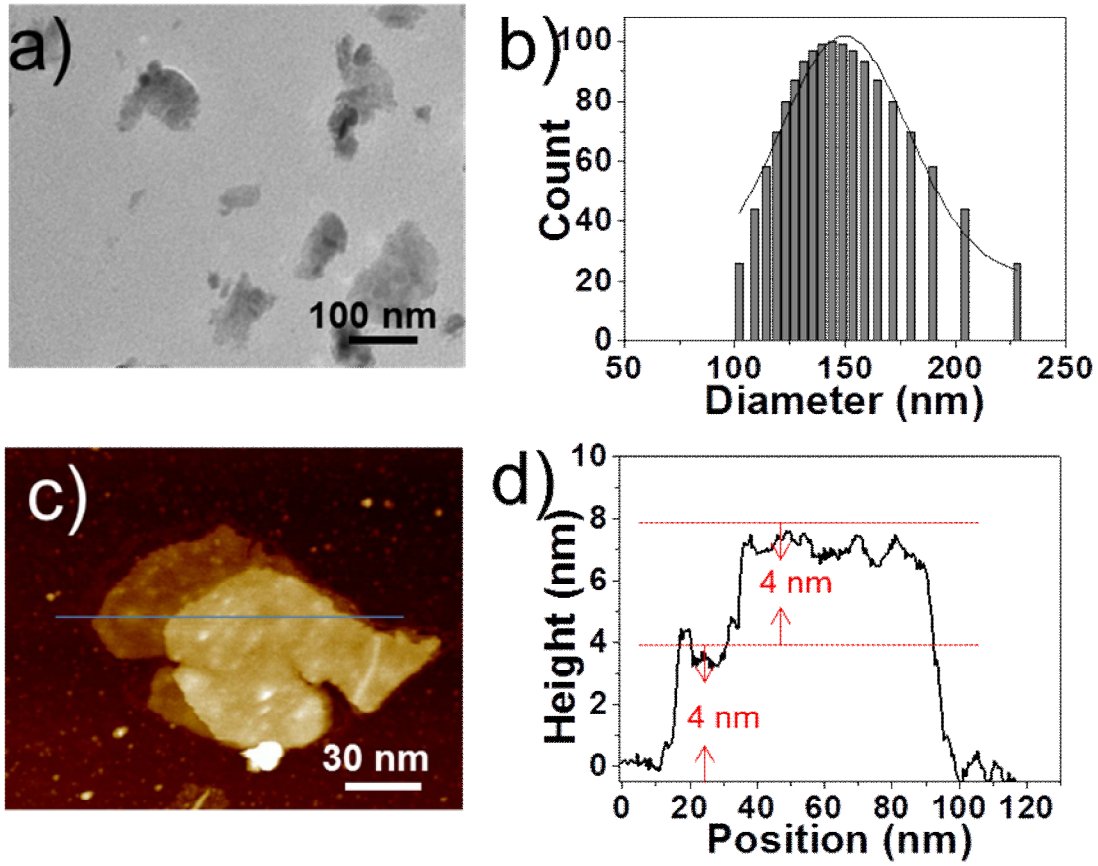

Figure S1. a) TEM image, **b)** size distribution, **c)** AFM image and **d)** thickness measured from c of the prepared 2D AM NSs.

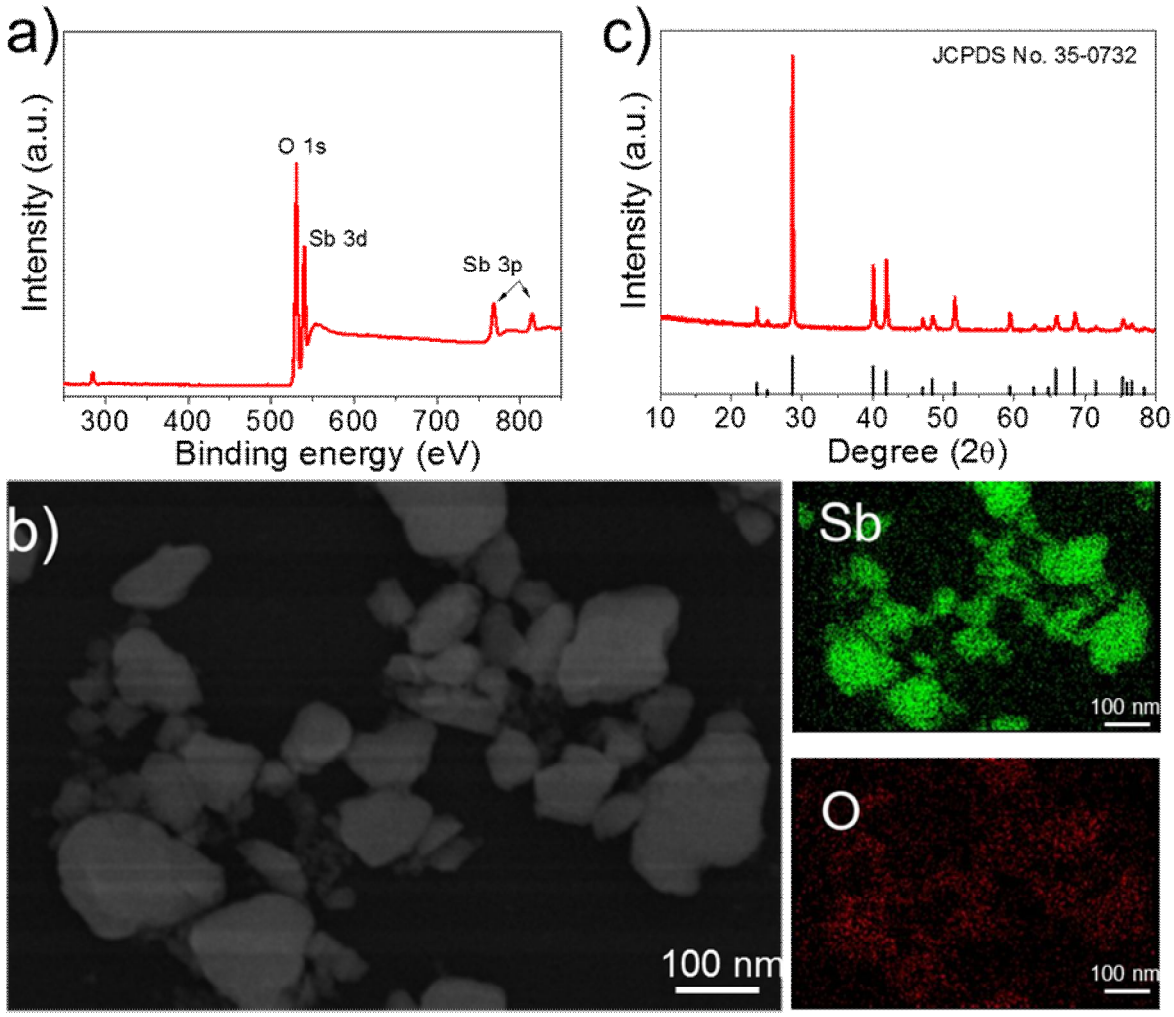

Figure S2. a) Full-scan XPS spectra of prepared AM NSs. **b)** STEM with EDC mapping images of AM NSs: Sb (green) and O (red). **c)** XRD pattern of prepared AM NSs.

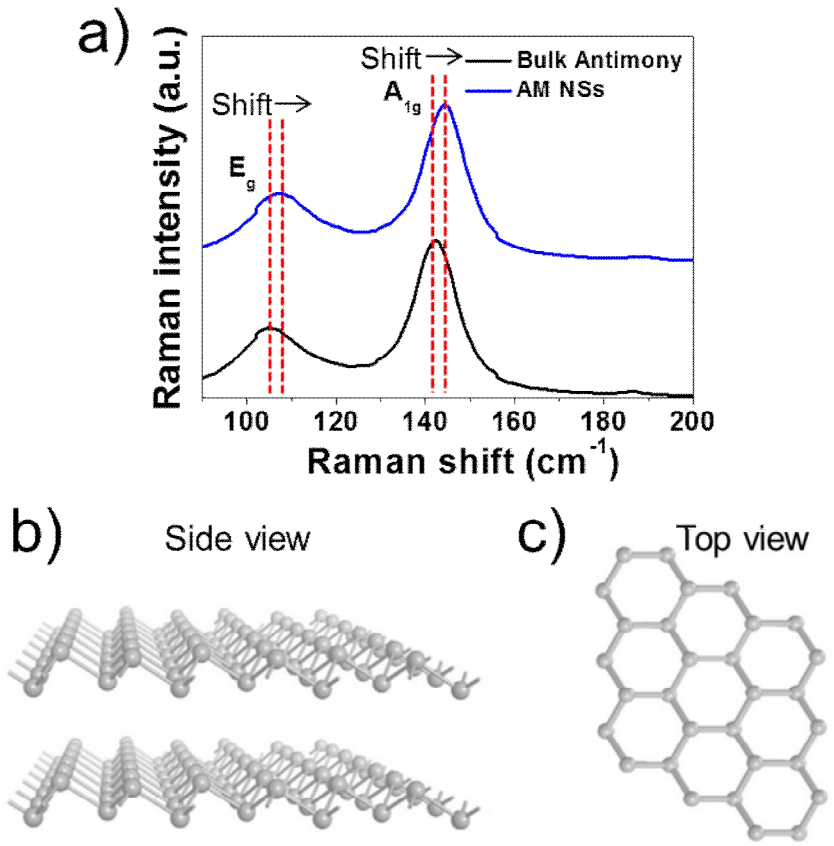

Figure S3. a) The Raman spectra of bulk antimony (Sb powder) and prepared AM NSs. Schematic representations of the atomic structure of the β-phase antimonene: **b)** side view and **c)** top view. The β-phase antimonene possesses a unique structure of interlinked ruffled hexagonal rings via strong interlayer Sb-Sb bonding and layer-to-layer weak interactions via van der Waals forces.

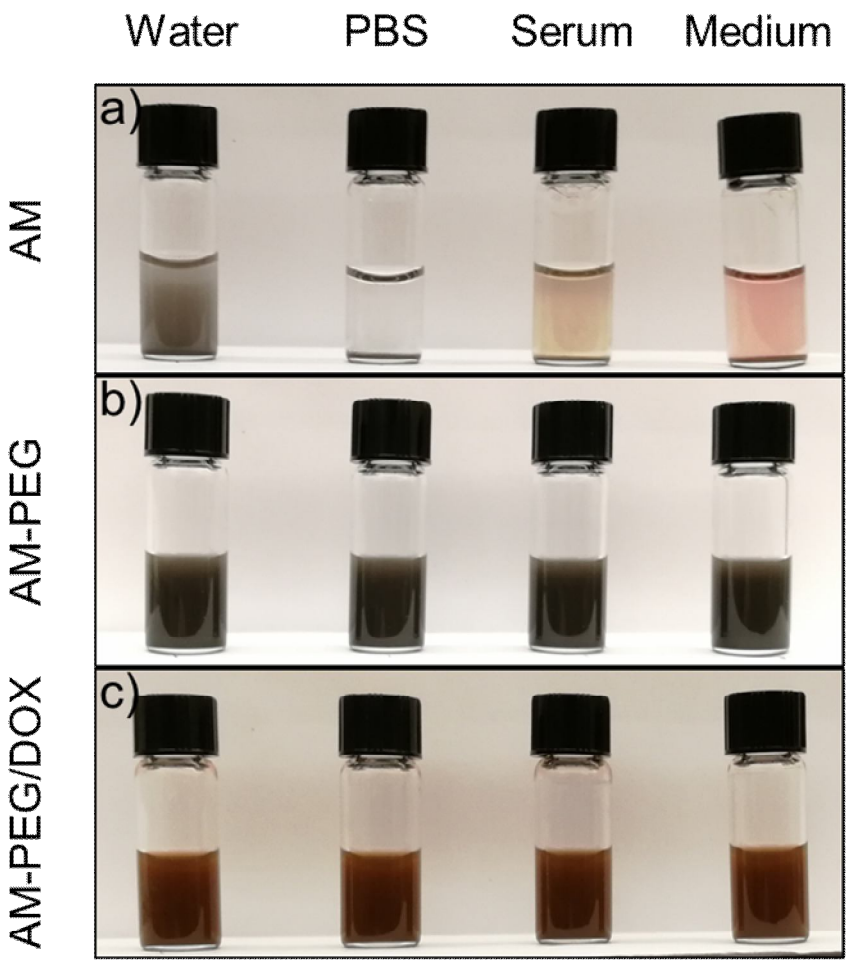

Figure S4. Photo images of the **a)** AM NSs, **b)** AM-PEG NSs, and **c)** AM-PEG/DOX NSs incubated in water, PBS, serum, or cell culture medium after 24 h.

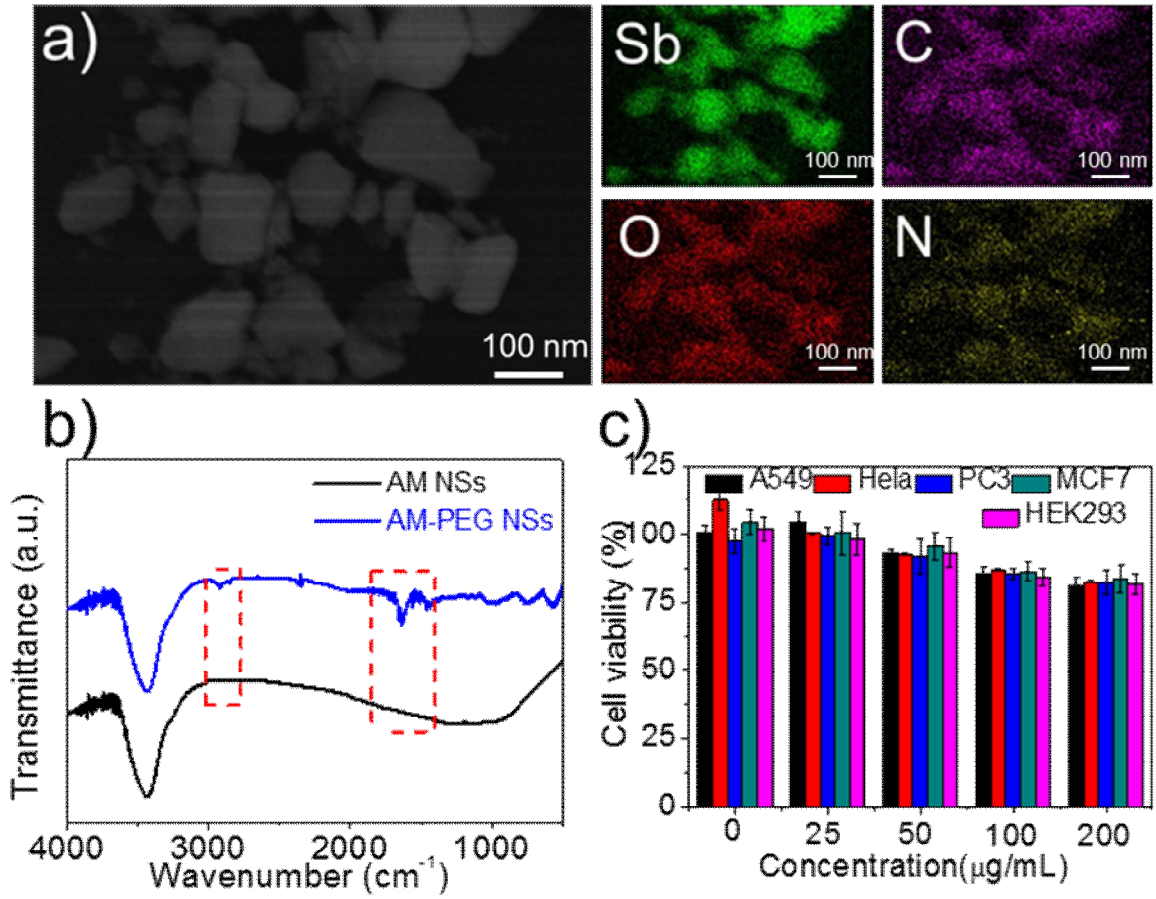

Figure S5. a) STEM with EDC mapping images of AM-PEG NSs: Sb (green), C (magenta), O (red), and N (yellow). **b)** FT-IR spectra of as-prepared AM and AM-PEG NSs. The absorption bands at ~2900 cm^{-1} belong to the CH vibration and ~1650 cm^{-1} was contributed by C=O stretching vibrations in the DSPE-PEG segment. **c)** Cell viability after incubation with AM-PEG NSs at various concentrations in different cell lines.

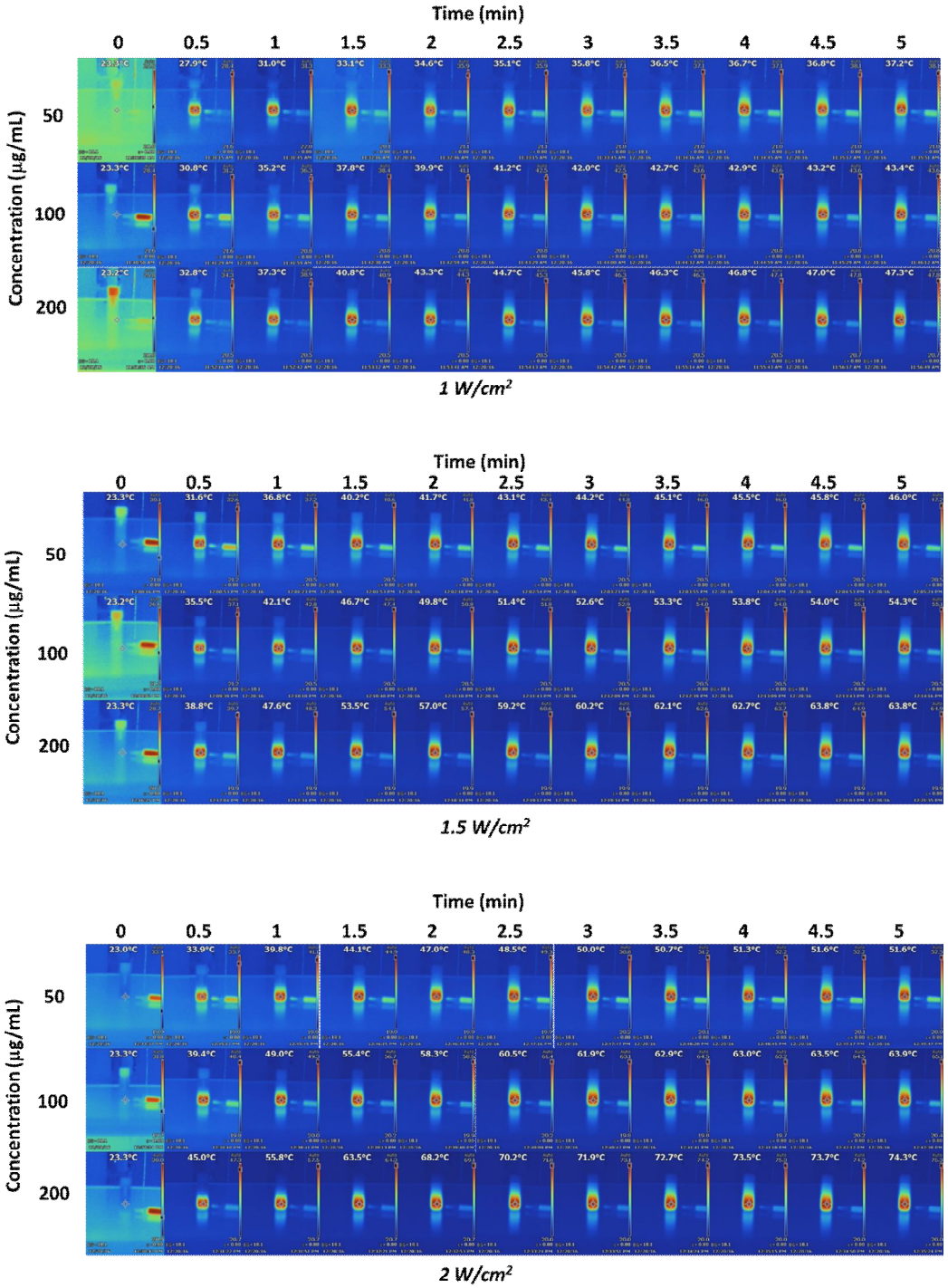

Figure S6. Thermal images of AM-PEG NSs aqueous solutions with different concentrations as a function of irradiation time for 5 min with different densities of an 808 nm NIR laser.

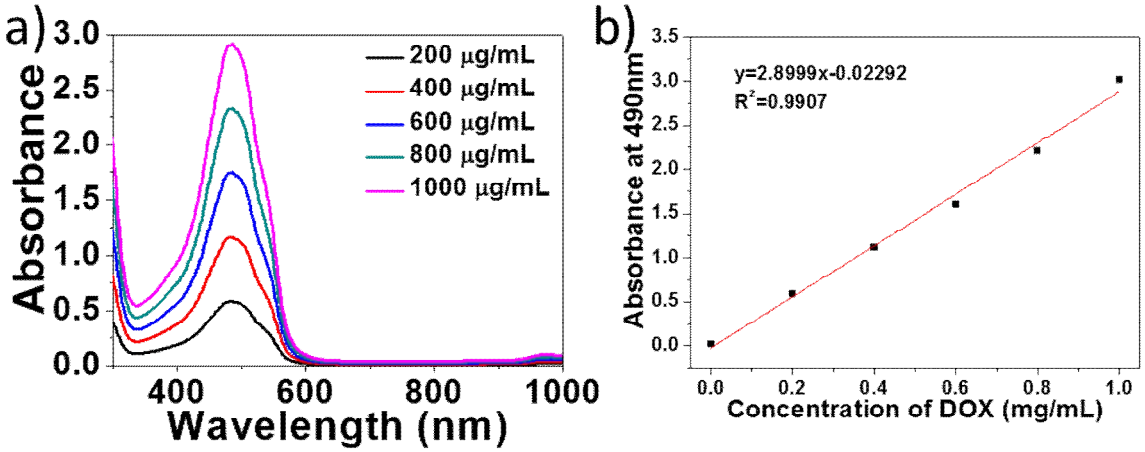

Figure S7. a) Absorbance spectra of DOX in water at different concentrations. **b)** Normalized absorbance intensity of DOX divided by the characteristic length of the cell (A/L) at different concentrations (λ = 490 nm).

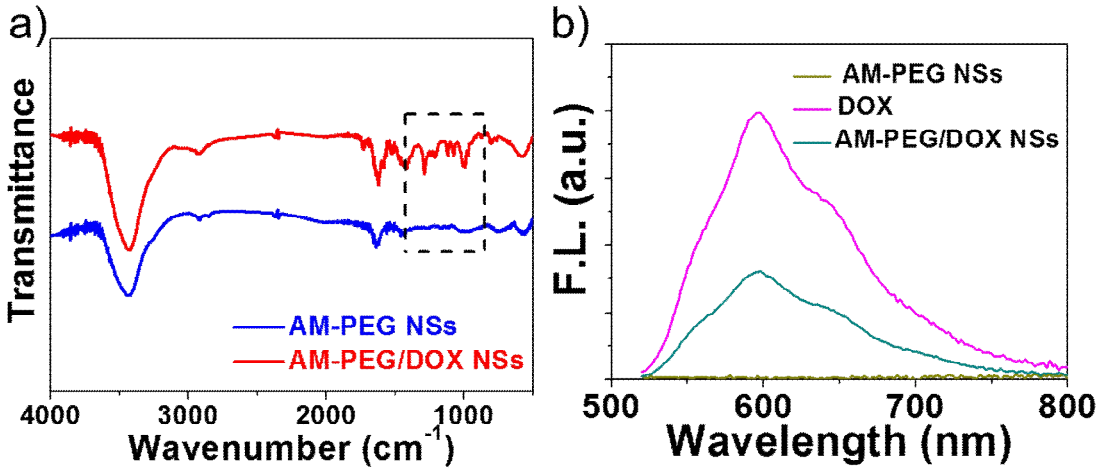

Figure S8. a) FT-IR spectrum of prepared AM-PEG and AM-PEG/DOX NSs. **b)** Fluorescence quenching of DOX molecules after loading on the AM-PEG NSs (λ = 490 nm).

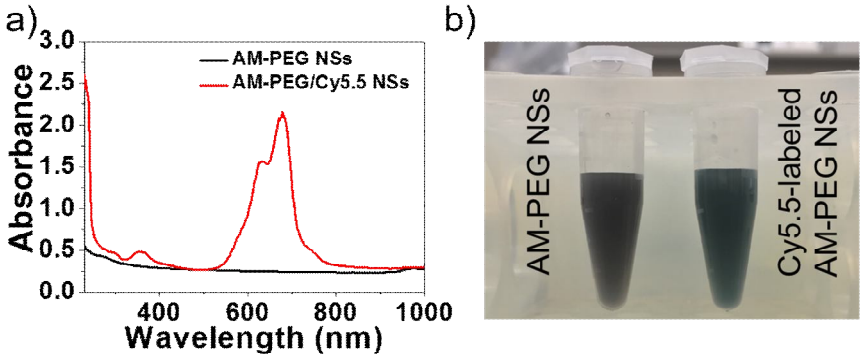

Figure S9. a) Absorbance spectra of purified AM-PEG NSs and AM-PEG-Cy5.5 NSs (λ = 675 nm). b) Photographs of the AM-PEG NSs and AM-PEG-Cy5.5 NSs.

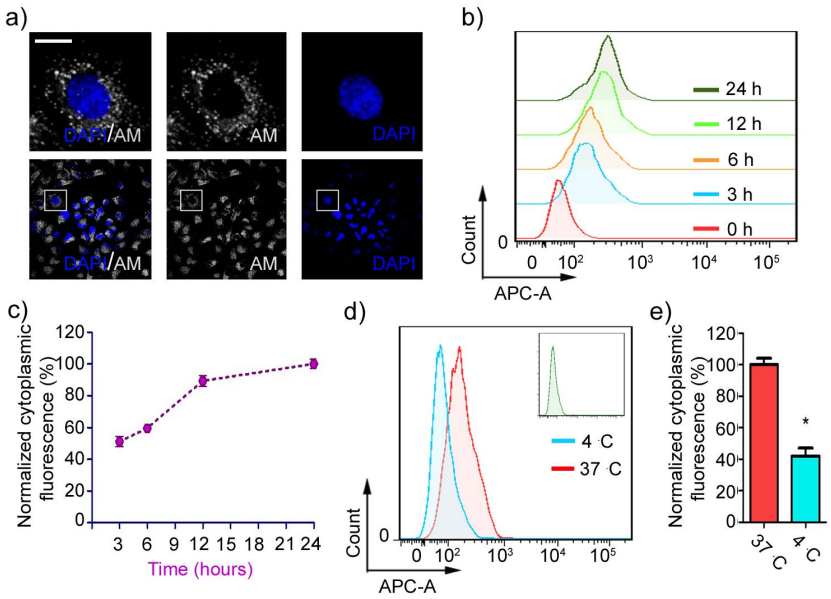

Figure S10. The effect of temperature on Cy5.5-labeled AM-PEG NSs' uptake in MCF-7 cells. **a)** The uptake of fluorescent AM-PEG NSs was tested by confocal laser scanning microscopy (CLSM) after 2 h of incubation. The images in the top row are enlarged versions of the white boxes in the second row (Scale bars: 10 μm). **b)** The uptake of AM-PEG NSs was measured by flow cytometer after indicated incubation times. **c)** Statistical analysis of intracellular fluorescence at indicated incubation times. **d)** Effect of temperature (37 °C and 4 °C) on AM-PEG NSs' uptake after 2 h-incubation, measured by flow cytometer. Statistical analysis of intracellular fluorescence in MCF-7 cells incubated at 37 °C and 4 °C, respectively.

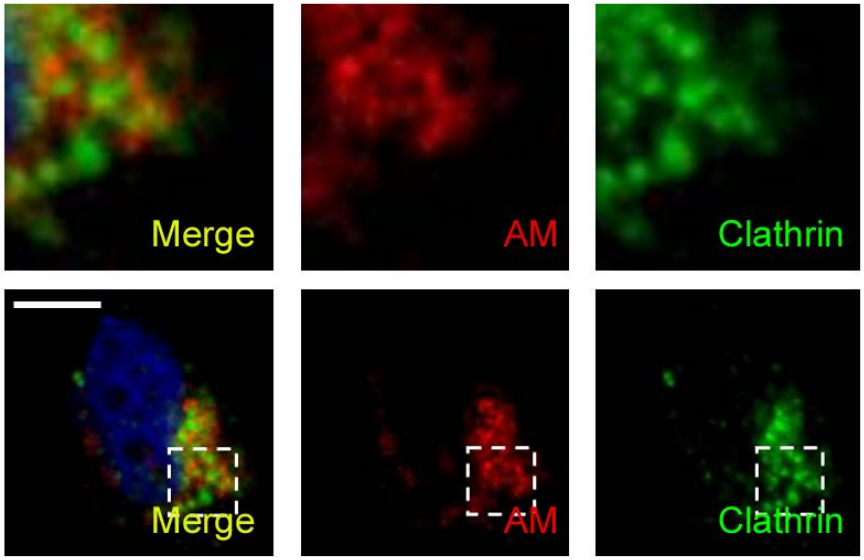

Figure S11. CLSM images of MCF-7 cells treated with Cy5.5-labeled AM-PEG NSs. Clathrin detected with primary antibody against Clathrin (Scale bars: 10 μm).

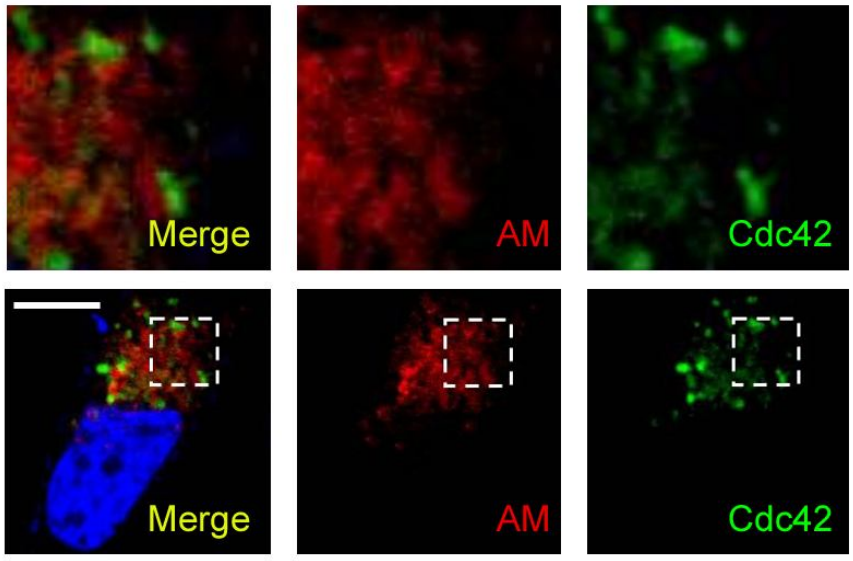

Figure S12. CLSM images of MCF-7 cells treated with Cy5.5-labeled AM-PEG NSs. Cdc42 detected with primary antibody against Cdc42 (Scale bars: 10 μm).

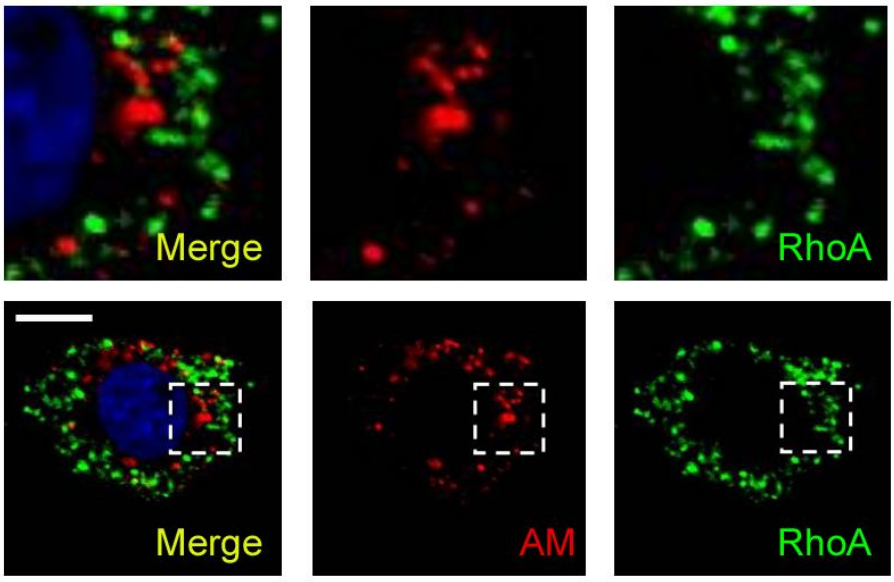

Figure S13. CLSM images of MCF-7 cells treated with Cy5.5-labeled AM-PEG NSs. RhoA detected with primary antibody against RhoA (Scale bars: 10 μm).

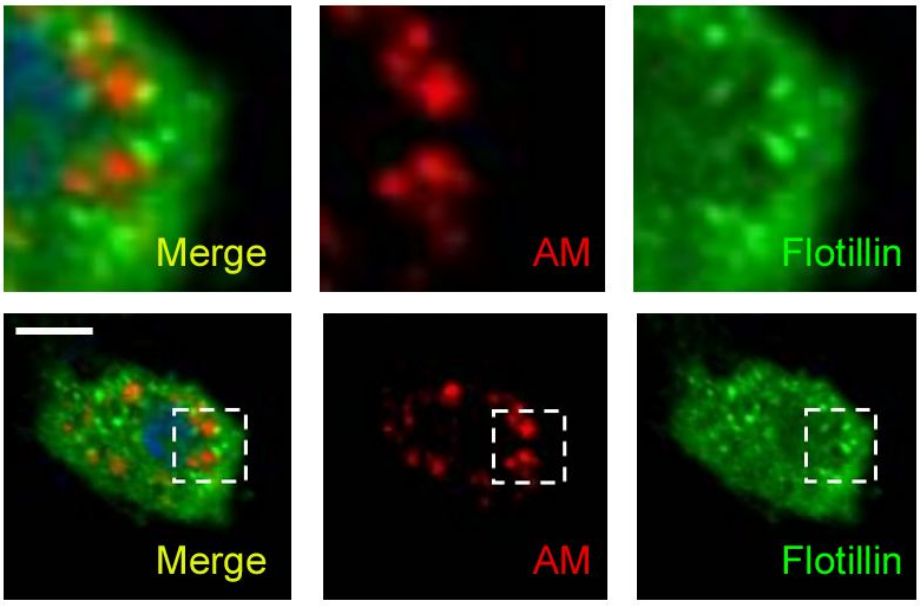

Figure S14. CLSM images of MCF-7 cells treated with Cy5.5-labeled AM-PEG NSs. Flotillin detected with primary antibody against Flotillin (Scale bars: 10 μm).

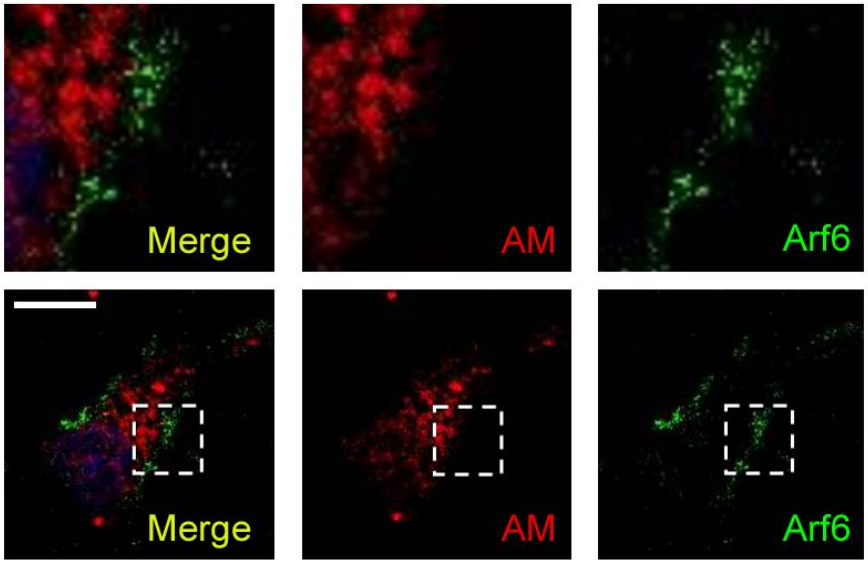

Figure S15. CLSM images of MCF-7 cells treated with Cy5.5-labeled AM-PEG NSs. Arf6 detected with primary antibody against Arf6 (Scale bars: 10 μm).

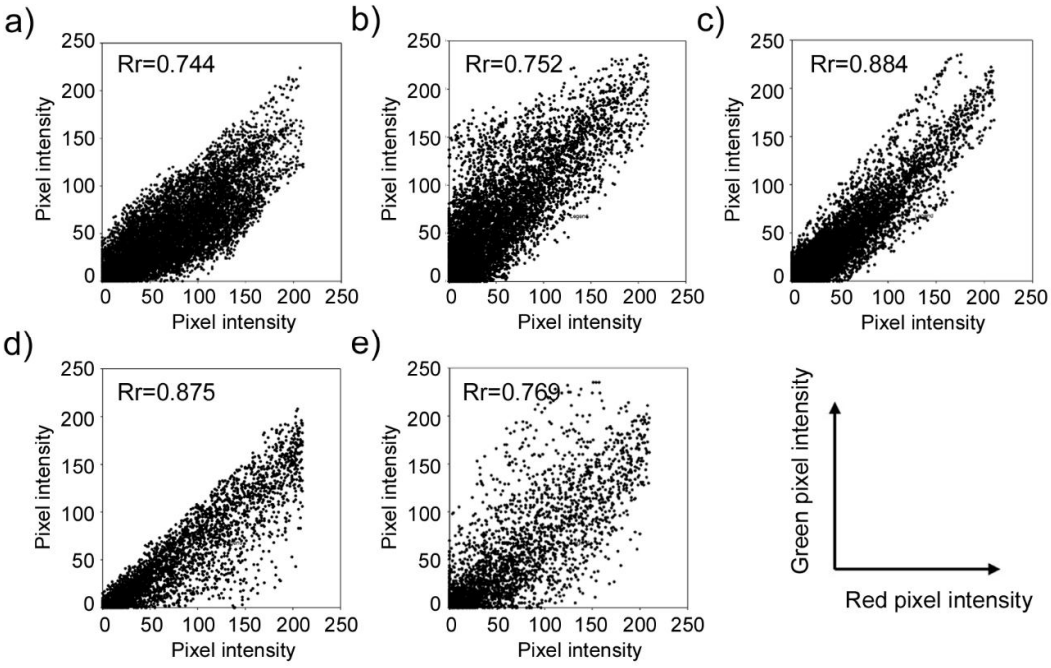

Figure S16. Scatterplot of red and green pixel intensities of the cells shown in **a)** Figure 2a, **b)** Figure 2b, **c)** Figure 2e, **d)** Figure 2f, and **e)** Figure 2g.

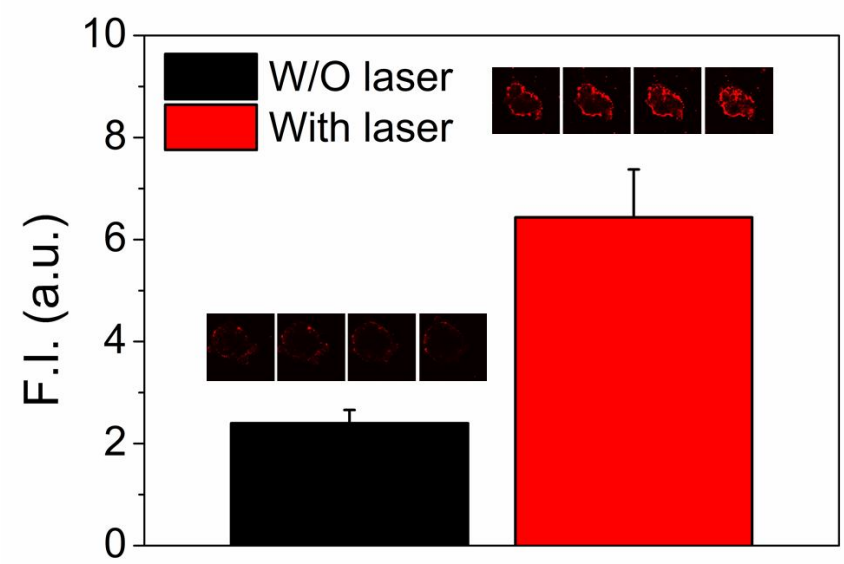

Figure S17. Average fluorescence intensity of four middle slices of the tumor spheroids from the without-(W/O) and with-laser irradiation groups.

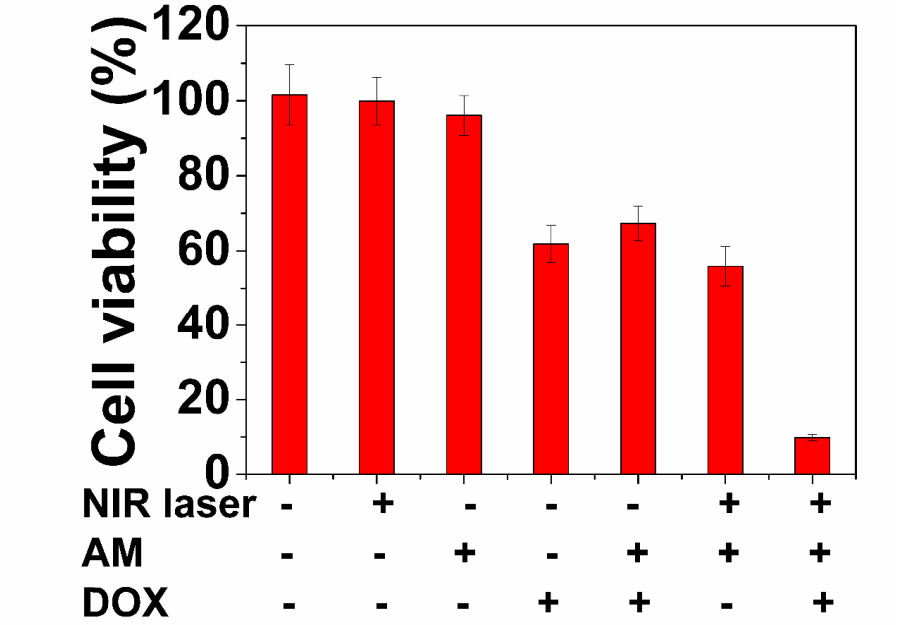

Figure S18. Cytotoxicity assays of PC3 cells in the presence of PBS, DOX, AM-PEG NSs, and AM-PEG/DOX NSs with or without irradiation.

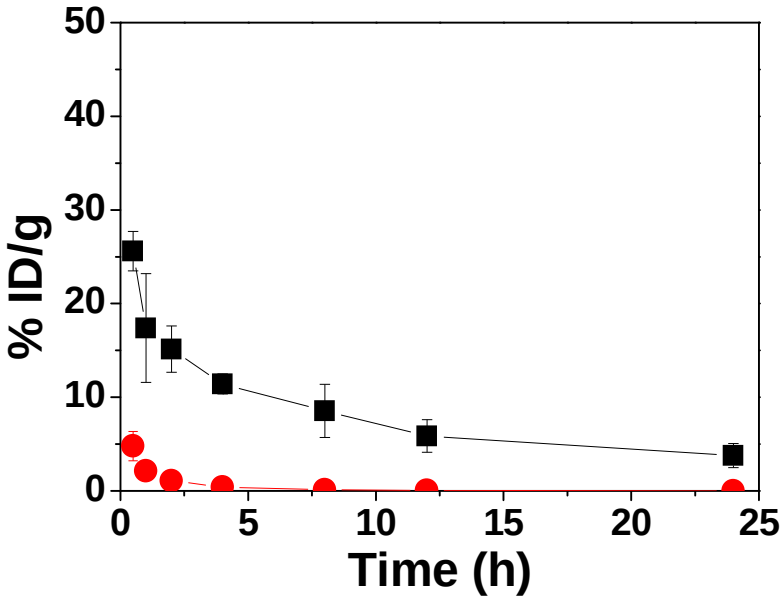

Figure S19. Blood circulation of free DOX and AM-PEG/DOX NSs after *i.v.* injection. The absorption peaks at 490 nm were used to determine DOX concentration, after the absorbance contributed from background and AM-PEG NSs were subtracted from the spectra.

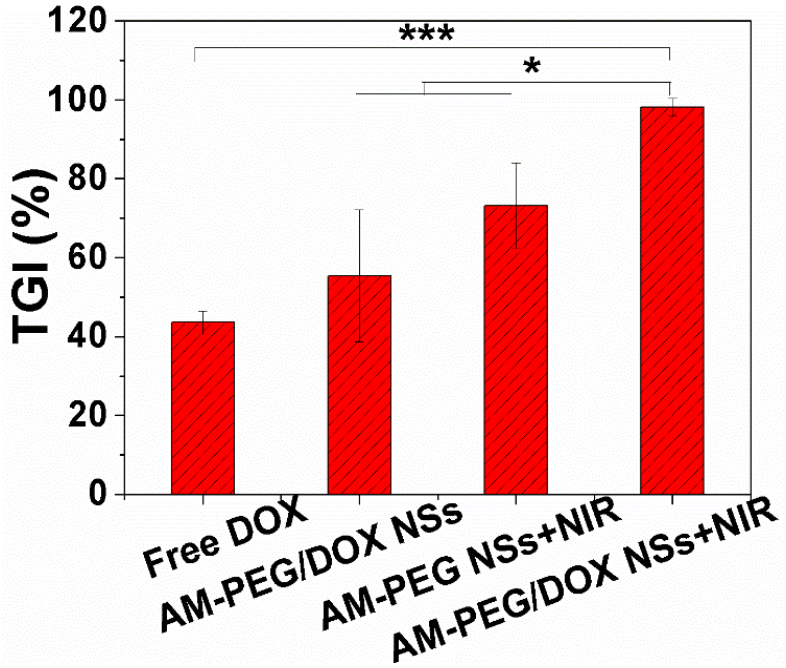

Figure S20. Tumor growth inhibition (TGI) rate in all groups at the end of different treatments compared to the control group.

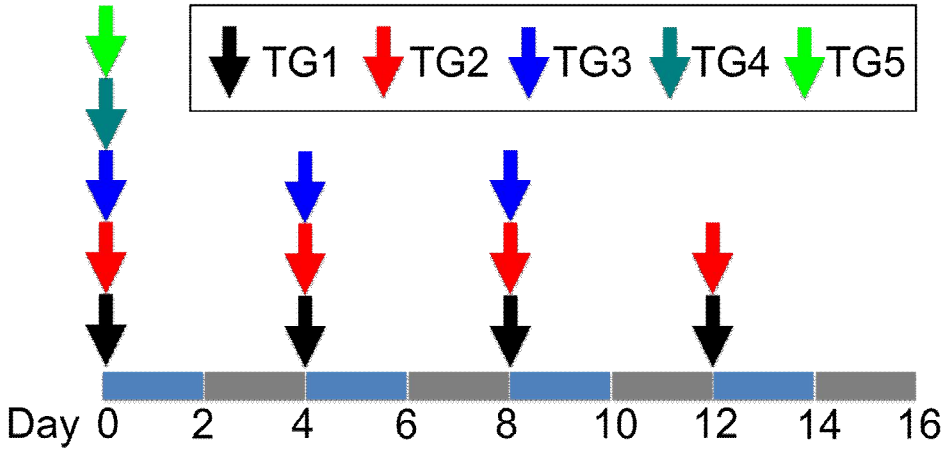

Figure S21. The number of treatments in different groups. The arrows indicate the timeline for different treatments. TG1: saline treatment in Group 1; TG2: DOX treatment in Group 2; TG3: AM-PEG/DOX NSs treatment in Group 3; TG4: AM-PEG NSs + NIR treatment in Group 4; TG5: AM-PEG/DOX NSs + NIR in Group 5.

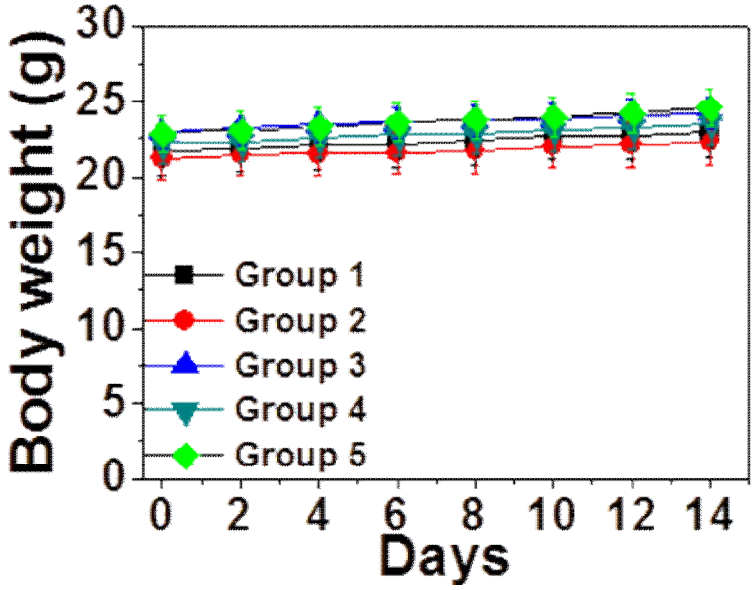

Figure S22. Body weight of mice in different groups during treatment. Group 1: Saline; Group 2: DOX; Group 3: AM-PEG/DOX NSs; Group 4: AM-PEG NSs + NIR; Group 5: AM-PEG/DOX NSs + NIR.

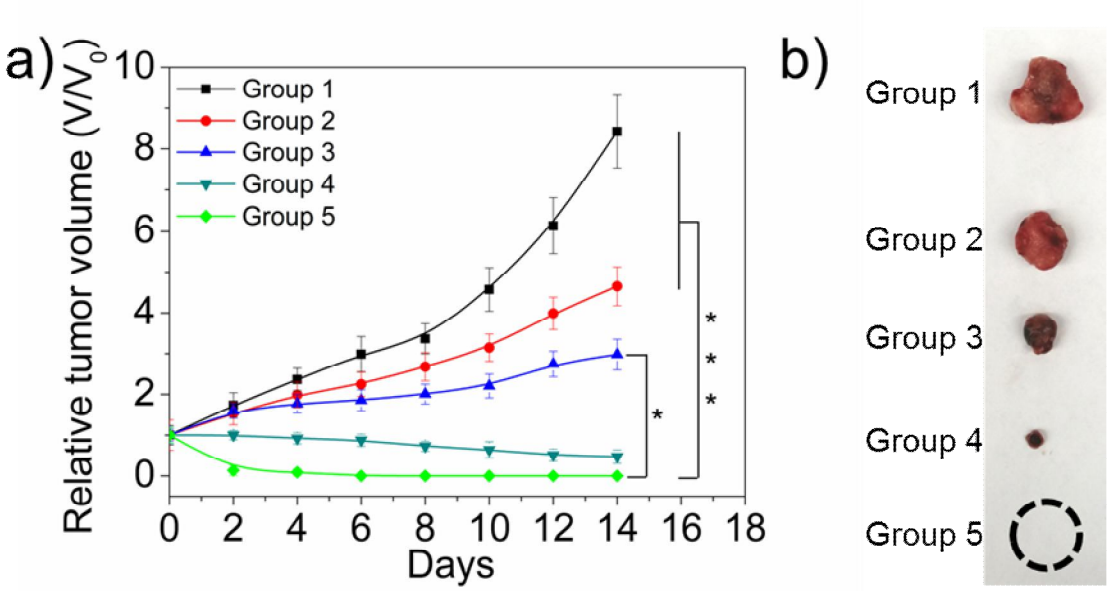

Figure S23. *In vivo* antitumor efficacy treated with low doses of therapeutics through intratumoral (*i.t.*) injection ([AM]= 1 mg/kg, [DOX] = 1 mg/kg). **a)** Growth curves of MCF-7 tumor-bearing nude mice after different treatments (*P < 0.05, ***P < 0.001). **b)** Digital photo of representative tumors in different groups after 14 days treatment. Group 1: saline; Group 2: DOX; Group 3: AM-PEG/DOX NSs; Group 4: AM-PEG NSs + NIR; Group 5: AM-PEG/DOX NSs + NIR. NIR laser irradiation was performed in Groups 4 and 5 for 10 min (0.8 W/cm^2, 808 nm) after *i.t.* injection.

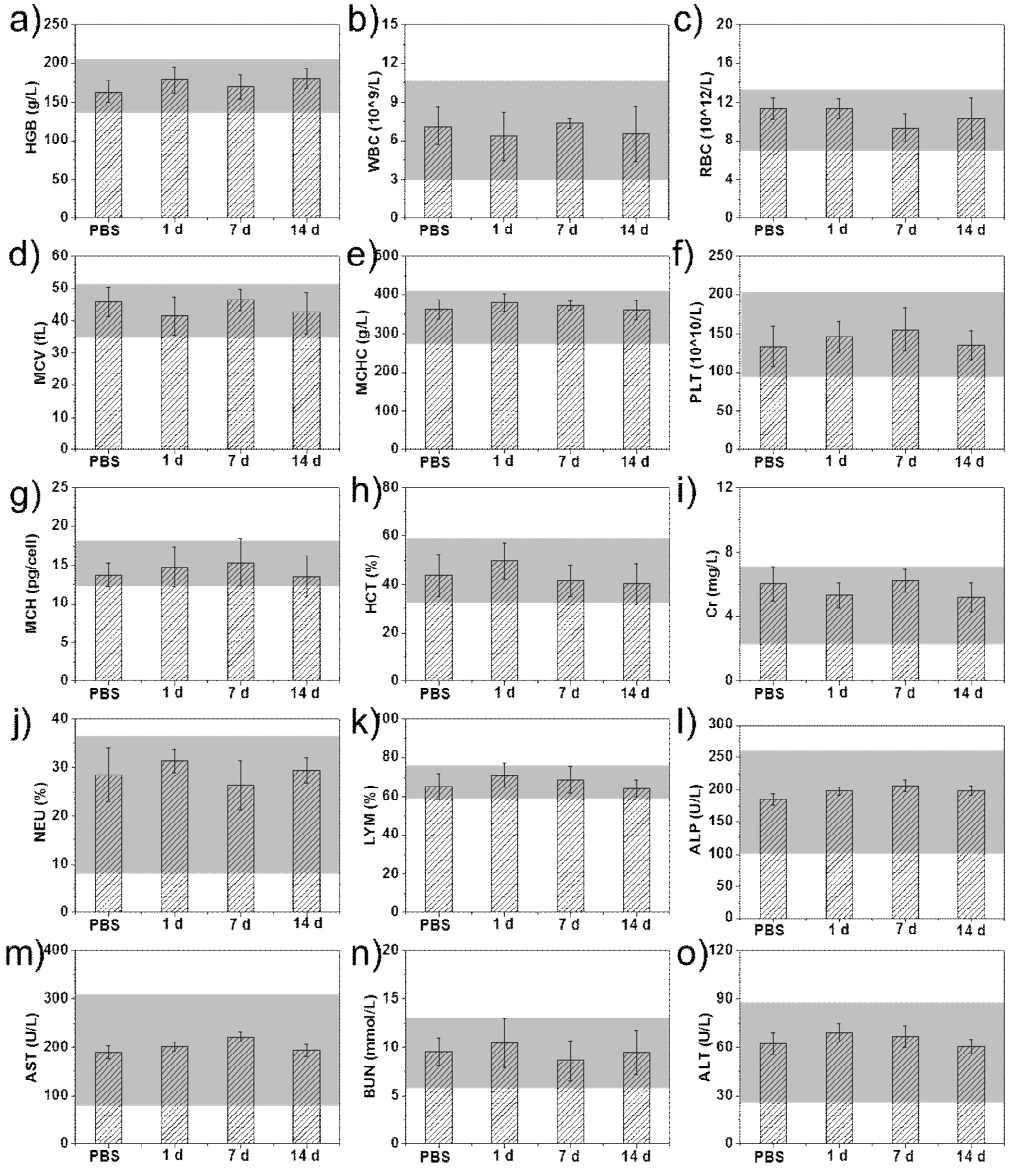

Figure S24. Blood biocompatibility tested in Balb/c mice treated with AM-based NSs. The complete blood parameters were assessed at different time points (1, 7, and 30 days): **a)** hemoglobin (HGB), **b)** white blood cells (WBC), **c)** red blood cells (RBC), **d)** mean corpuscular volume (MCV), **e)** mean corpuscular hemoglobin concentration (MCHC), **f)** platelet (PLT), **g)** mean corpuscular hemoglobin (MCH), **h)** hematocrit (HCT), **i)** creatinine (Cr), **j)** neutral cell percentage (NEU%), **k)** lymphocyte percentage (LYM%), **l)** alkaline phosphatase (ALP), **m)** aspartate aminotransferase (AST), **n)** urea nitrogen (BUN), **o)** alanine aminotransferase (ALT).

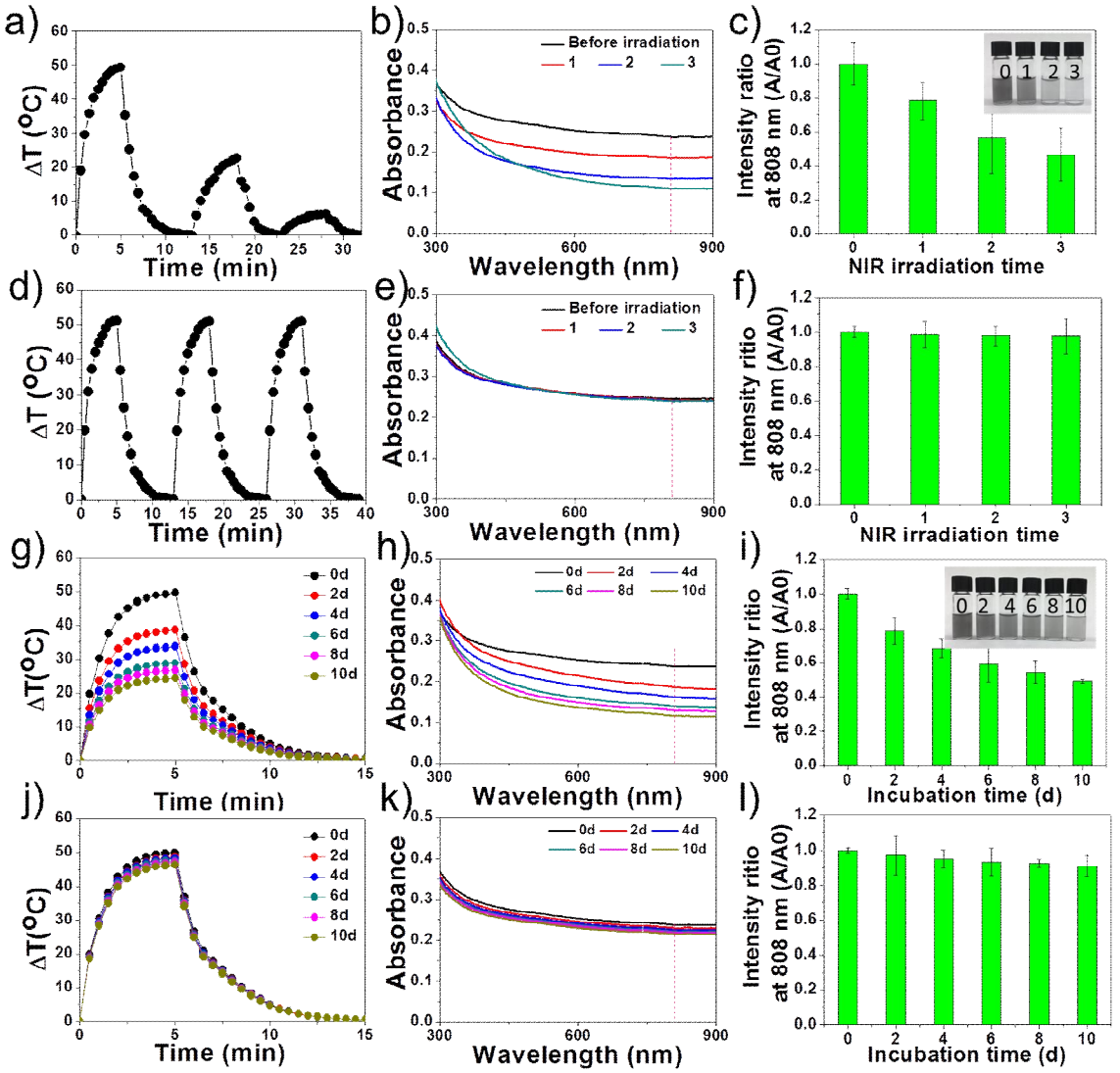

Figure S25. Degradation of AM-based NSs. **a)** Heating of a suspension of AM NSs in water for three heating-cooling cycles under 808-nm NIR laser irradiation. **b)** Absorbance spectra and **c)** Variation of the absorption ratios at 808 nm (A/A_0%) of prepared AM NSs in water after different irradiation cycles in (a); **d)** Heating of a suspension of AM NSs in ethanol for three heating-cooling cycles under an 808 nm NIR laser irradiation. **e)** Absorbance spectra and **f)** Variation of the absorption ratios at 808 nm (A/A_0%) of AM NSs in ethanol after different irradiation cycles in (d); **g)** Time-dependent temperature changes (under an 808 nm NIR laser irradiation) of water suspensions of AM NSs after different days of incubation in an oxygen atmosphere. **h)** Absorbance spectra and **i)** Variation of the absorption ratios at 808 nm (A/A_0%) of AM NSs in water after different days of incubation in (g); **j)** Time-dependent temperature

changes (under an 808 nm NIR laser irradiation) of water suspensions of AM NSs after different periods of incubation in an oxygen-free environment. **k)** Absorbance spectra and **l)** Variation of the absorption ratios at 808 nm (A/A_0%) of AM NSs in water after different periods of incubation in (j). The power density of NIR laser was 2 W/cm^2.

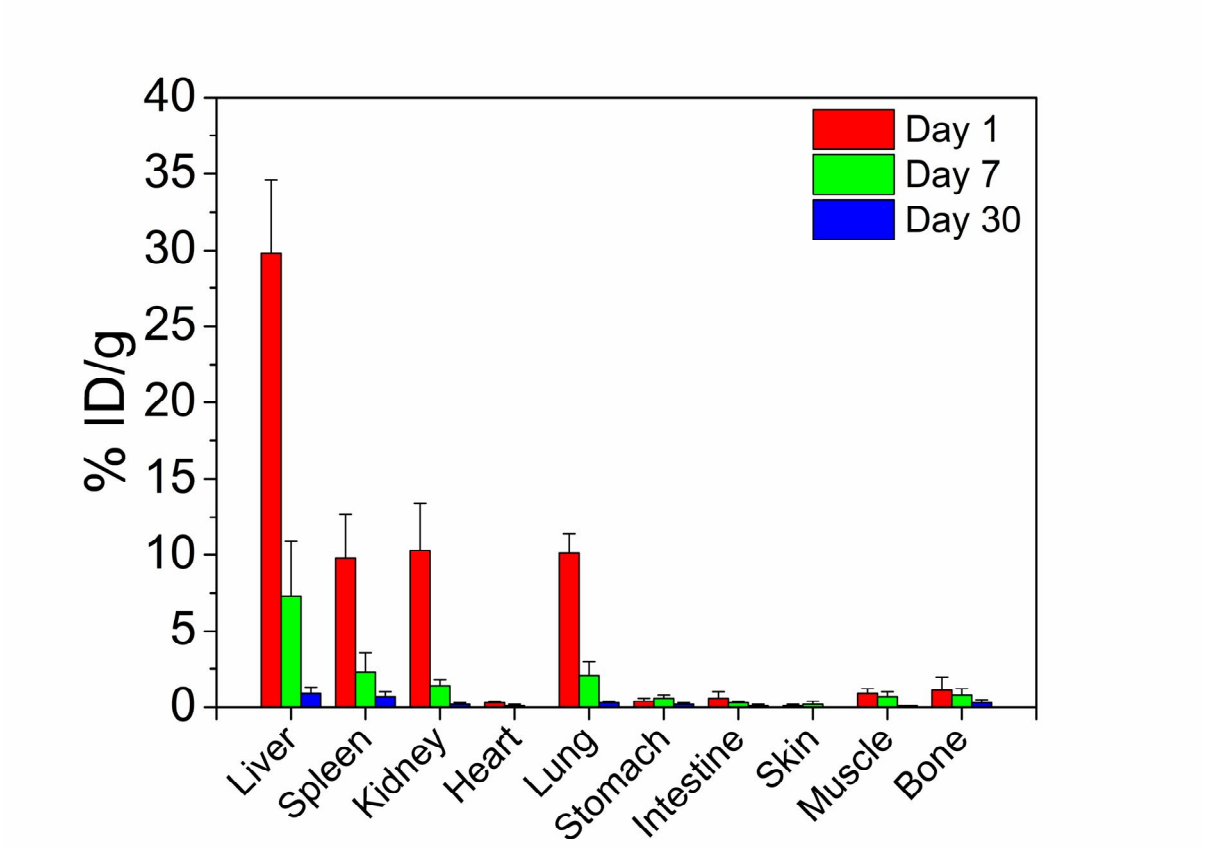

Figure S26. Biodistribution of AM-based NSs in different organs 1, 7, or 30 days after intravenous injection (n = 5). %ID/g = percentage of the injected dose per gram of tissue.

Supplementary References

[1] C. Gibaja, D. Rodriguez-San-Miguel, P. Ares, J. Gomez-Herrero, M. Varela, R. Gillen, J. Maultzsch, F. Hauke, A. Hirsch, G. Abellan, F. Zamora, *Angew Chem Int Ed* **2016**, 55, 14345.

[2] X. Wang, X. Zhen, J. Wang, J. Zhang, W. Wu, X. Jiang, *Biomaterials* **2013**, 34, 4667.

[3] W. Tao, X. Zhu, X. Yu, X. Zeng, Q. Xiao, X. Zhang, X. Ji, X. Wang, J. Shi, H. Zhang, L. Mei, *Adv Mater* **2017**, 29, 1603276.

[4] W. Tao, X. Ji, X. Xu, M. A. Islam, Z. Li, S. Chen, P. E. Saw, H. Zhang, Z. Bharwani, Z. Guo, J. Shi, O. C. Farokhzad, *Angew Chem Int Ed* **2017**, 56, 11896.

[5] a) Y. Yokoyama, M. Dhanabal, A. W. Griffioen, V. P. Sukhatme, S. Ramakrishnan, *Cancer Res* **2000**, 60, 2190; b) Z. Jin-Rong, Y. Lunyin, M. Zhiming, B. G. L., *Int J Cancer* **2004**, 108, 8.

[6] a) F. Frezard, C. Demicheli, R. R. Ribeiro, *Molecules* **2009**, 14, 2317; b) Y. A. Kuryshev, L. Wang, B. A. Wible, X. Wan, E. Ficker, *Mol Pharmacol* **2006**, 69, 1216.

[7] F. Flury, *N Naunyn Schmiedebergs Arch Exp Pathol Pharmakol* **1927**, 126, 87.

[8] E. Bomhard, E. Loser, A. Dornemann, B. Schilde, *Toxicol Lett* **1982**, 14, 189.

[9] L. Friberg, G. Nordberg, V. B. Vouk, *Handbook on the toxicology of metals*, Elsevier/North-Holland Biomedical Press; sole distributors for the U.S.A. and Canada, Amsterdam; New York 1979.

[10] L. F. James, V. A. Lazar, W. Binns, *Am J Vet Res* **1966**, 27, 132.

[11] J. B. Casals, *Br J Pharmacol* **1972**, 46, 281.

[12] K. A. Winship, *Adverse Drug React Acute Poisoning Rev* **1987**, 6, 67.